

Published in final edited form as:

Nature. ; 486(7403): 400–404. doi:10.1038/nature11017.

The landscape of cancer genes and mutational processes in breast cancer

Philip J. Stephens^{1,*}, Patrick S. Tarpey^{1,*}, Helen Davies¹, Peter Van Loo^{1,2}, Chris Greenman^{1,3,4}, David C. Wedge¹, Serena Nik-Zainal¹, Sancha Martin¹, Ignacio Varela¹, Graham R. Bignell¹, Lucy R. Yates^{1,5,6}, Elli Papaemmanuil¹, David Beare¹, Adam Butler¹, Angela Cheverton¹, John Gamble¹, Jonathan Hinton¹, Mingming Jia¹, Alagu Jayakumar¹, David Jones¹, Calli Latimer¹, King Wai Lau¹, Stuart McLaren¹, David J. McBride¹, Andrew Menzies¹, Laura Mudie¹, Keiran Raine¹, Roland Rad¹, Michael Spencer Chapman¹, Jon Teague¹, Douglas Easton^{7,8}, Anita Langerød⁹, OSBREAC[†], Ming Ta Michael Lee¹⁰, Chen-Yang Shen¹⁰, Benita Tan Kiat Tee¹¹, Bernice Wong Huimin¹², Annegien Broeks¹³, Ana Cristina Vargas¹⁴, Gulisa Turashvili^{15,16}, John Martens¹⁷, Aquila Fatima¹⁸, Penelope Miron¹⁸, Suet-Feung Chin¹⁹, Gilles Thomas²⁰, Sandrine Boyault²⁰, Odette Mariani²¹, Sunil R. Lakhani^{14,22,23}, Marc van de Vijver²⁴, Laura van 't Veer¹³, John Foekens¹⁷, Christine Desmedt²⁵, Christos Sotiriou²⁵, Andrew Tutt⁵, Carlos Caldas^{19,26}, Jorge S. Reis-Filho²⁷, Samuel A. J. R. Aparicio^{15,16}, Anne Vincent Salomon^{21,28}, Anne-Lise Børresen-Dale^{9,29}, Andrea L. Richardson^{18,30}, Peter J. Campbell^{1,31,32}, P. Andrew Futreal¹, and Michael R. Stratton¹

¹Cancer Genome Project, Wellcome Trust Sanger Institute, Wellcome Trust Genome Campus, Hinxton CB10 1SA, UK ²Human Genome Laboratory, Department of Human Genetics, VIB and University of Leuven, Herestraat 49 Box 602, B-3000 Leuven, Belgium ³School of Computing Sciences, University of East Anglia, Norwich NR4 7TJ, UK ⁴The Genome Analysis Centre, Norwich Research Park, Norwich NR4 7UH, UK ⁵Breakthrough Breast Cancer Research Unit, Research Oncology, 3rd Floor Bermondsey Wing, Guy's Hospital Campus, Kings College London School of Medicine, London SE1 9RT, UK ⁶Department of Clinical Oncology, Ground floor, Lambeth Wing, Guys and St Thomas' NHS Trust, Westminster Bridge Road, London SE1 7EH, UK ⁷Centre for Cancer Genetic Epidemiology, Department of Oncology, Strangeways Research Laboratory, Cambridge CB1 8RN, UK ⁸Centre for Cancer Genetic Epidemiology, Department of Public Health and Primary Care, Strangeways Research Laboratory, Cambridge CB1 8RN, UK ⁹Department of Genetics, Institute for Cancer Research, The Norwegian Radium Hospital, Oslo

©2012 Macmillan Publishers Limited. All rights reserved

*These authors contributed equally to this work.

†Lists of participants and their affiliations appear at the end of the paper.

Supplementary Information is linked to the online version of the paper at www.nature.com/nature.

Author Contributions P.J.S., P.S.T. and H.D. performed analysis of the sequence data, aided by S.N.Z., I.V., G.R.B., L.R.Y., E.P., D.J.M., M.S.-C. and R.R. P.V.L. performed analysis of the SNP6 data. C.G., D.C.W., K.W.L. and D.E. performed the statistical investigations. S. Martin coordinated sample acquisition and pathology review. S. McLaren coordinated sample processing. D.B., A. Butler, J.G., J.H., M.J., A.J., D.J., A.M., K.R. and J.T. performed informatics investigations. A.C., C.L. and L.M. performed technical investigations. A.L., OSBREAC, M.T.M.L., C.-Y.S., B.T.K.T., B.W.H., A. Broeks, A.C.V., G. Turashvili, J.M., A.F., P.M., S.-F.C., G. Thomas, S.B., O.M., S.R.L., M.v.d.V., L.v.'t.V., J.F., C.D., C.S., A.T., C.C., J.S.R.-F., S.A.J.R.A., A.V.S., A.-L.B.-D. and A.R. contributed samples, clinical data and scientific advice. P.J.C. and P.A.F. directed the research and contributed to the manuscript. M.R.S. directed the research and wrote the manuscript.

Author Information Genome sequence data have been deposited at the European Genome-phenome Archive under accession number EGAD00001000133. Affymetrix SNP6 data have been deposited under accession number E-MTAB-1110. Reprints and permissions information is available at www.nature.com/reprints. The authors declare no competing financial interests. Readers are welcome to comment on the online version of this article at www.nature.com/nature. Correspondence and requests for materials should be addressed to M.R.S. (mrs@sanger.ac.uk).

University Hospital, O310 Oslo, Norway ¹⁰National Genotyping Center, Institute of Biomedical Sciences, Academia Sinica, 128 Academia Road, Sec 2, Nankang, Taipei 115, Taiwan, China ¹¹Department of General Surgery, Singapore General Hospital, 169608, Singapore ¹²NCCS-VARI Translational Research Laboratory, National Cancer Centre Singapore, 11 Hospital Drive, 169610, Singapore ¹³Department Experimental Therapy, The Netherlands Cancer Institute, Plesmanlaan 121, 1066 CX Amsterdam, The Netherlands ¹⁴The University of Queensland Centre for Clinical Research, The Royal Brisbane & Women's Hospital, Herston, Brisbane, Queensland 4029, Australia ¹⁵Department of Pathology and Laboratory Medicine, University of British Columbia, Vancouver, British Columbia V6T 2B5, Canada ¹⁶Molecular Oncology, British Columbia Cancer Research Centre, Vancouver, British Columbia V5Z 1L3, Canada ¹⁷Department of Medical Oncology, Erasmus University Medical Center, Daniel den Hoed Cancer Center and Cancer Genomics Center, Postbus 2040, 3000 CA Rotterdam, Netherlands ¹⁸Department of Cancer Biology, Dana-Farber Cancer Institute, 450 Brookline Avenue, Boston, Massachusetts 02215, USA ¹⁹Department of Oncology, University of Cambridge and Cancer Research UK Cambridge Research Institute, Li Ka Shin Centre, Cambridge CB2 0RE, UK ²⁰Université Lyon 1, INCa-Synergie, Centre Leon Berard, 28 rue Laennec, Lyon CEDEX 08, France ²¹Institut Curie, Department of Tumor Biology, 26 rue d'Ulm, 75248 Paris CEDEX 05, France ²²The University of Queensland School of Medicine, Herston Road, Herston, Brisbane, Queensland 4006, Australia ²³Anatomical Pathology, Pathology Queensland, The Royal Brisbane and Women's Hospital, Herston, Brisbane, Queensland 4029, Australia ²⁴Department of Pathology, Academic Medical Center, Meibergdreef 9, 1105 AZ Amsterdam, The Netherlands ²⁵Breast Cancer Translational Laboratory, Université Libre de Bruxelles, Jules Bordet Institute, Boulevard de Waterloo 121, 1000 Brussels, Belgium ²⁶NIHR Cambridge Biomedical Research Centre and Cambridge Experimental Cancer Medicine Centre, Cambridge University Hospitals NHS Foundation Trust, Cambridge CB2 2QQ, UK ²⁷The Breakthrough Breast Cancer Research Centre, Institute of Cancer Research, London SW3 6JB, UK ²⁸Institut Curie, INSERM Unit 830, 26 rue d'Ulm, 75248 Paris CEDEX 05, France ²⁹K.G. Jebsen Center for Breast Cancer Research, Institute for Clinical Medicine, Faculty of Medicine, University of Oslo, O318 Oslo, Norway ³⁰Department of Pathology, Brigham and Women's Hospital, Harvard Medical School, 75 Francis St, Boston, Massachusetts 02115, USA ³¹Department of Haematology, Addenbrooke's Hospital, Cambridge CB2 0QQ, UK ³²Department of Haematology, University of Cambridge, Hills Road, Cambridge CB2 2XY, UK

Abstract

All cancers carry somatic mutations in their genomes. A subset, known as driver mutations, confer clonal selective advantage on cancer cells and are causally implicated in oncogenesis¹, and the remainder are passenger mutations. The driver mutations and mutational processes operative in breast cancer have not yet been comprehensively explored. Here we examine the genomes of 100 tumours for somatic copy number changes and mutations in the coding exons of protein-coding genes. The number of somatic mutations varied markedly between individual tumours. We found strong correlations between mutation number, age at which cancer was diagnosed and cancer histological grade, and observed multiple mutational signatures, including one present in about ten per cent of tumours characterized by numerous mutations of cytosine at TpC dinucleotides. Driver mutations were identified in several new cancer genes including *AKT2*, *ARID1B*, *CASP8*, *CDKN1B*, *MAP3K1*, *MAP3K13*, *NCOR1*, *SMARCD1* and *TBX3*. Among the 100 tumours, we found driver mutations in at least 40 cancer genes and 73 different combinations of mutated cancer genes. The results highlight the substantial genetic diversity underlying this common disease.

The coding exons of 21,416 protein coding genes and 1,664 microRNAs were sequenced and copy number changes examined in 100 primary breast cancers, 79 of which were

oestrogen receptor positive (ER+) and 21 of which were oestrogen receptor negative (ER-) (Supplementary Table 1). We sequenced normal DNAs from the same individuals to exclude inherited sequence variation. We identified 7,241 somatic point mutations: 6,964 were single-base substitutions, of which 4,737 were predicted to generate missense; 422, nonsense; 158, an essential splice site; 8, stop codon read-through; and 1,637, silent changes in protein sequence. Two substitutions were found in microRNAs. There were 277 small insertions or deletions (71 and 206, respectively), of which 231 introduced translational frameshifts and 46 were in-frame (Supplementary Table 2). Analyses of copy number yielded 1,712 homozygous deletions and 1,751 regions of increased copy number (amplification) (Supplementary Table 3).

Somatic driver substitutions and small insertions/deletions (indels) were identified in cancer genes previously implicated in breast cancer development, including *AKT1*, *BRCA1*, *CDH1*, *GATA3*, *PIK3CA*, *PTEN*, *RBI* and *TP53* (Supplementary Table 4; see also <http://www.sanger.ac.uk/genetics/CGP/Census>). Likely drivers were also found in cancer genes involved in other cancer types, including *APC*, *ARID1A*, *ARID2*, *ASXL1*, *BAP1*, *KRAS*, *MAP2K4*, *MLL2*, *MLL3*, *NF1*, *SETD2*, *SF3B1*, *SMAD4* and *STK11*.

To identify new cancer genes, we searched for non-random clustering of somatic mutations in each of the 21,416 protein-coding genes^{2,3} and sequenced a subset of genes highlighted by this analysis in a followup series of 250 breast cancers (Supplementary Tables 5 and 6). Persuasive evidence was found for nine new cancer genes (Fig. 1a and Supplementary Fig. 1). Of these *ARID1B*, *CASP8*, *MAP3K1*, *MAP3K13*, *NCOR1*, *SMARCD1* and *CDKN1B* had the truncating mutations and often biallelic inactivation characteristic of inactivated, potentially recessive cancer genes (Supplementary Table 4). *AKT2* is probably an activated, dominantly acting cancer gene. The effects of *TBX3* mutations on its function are unclear.

MAP3K1 encodes a serine/threonine protein kinase that regulates the activity of the ERK MAP kinase (the extracellular signal-regulated mitogen-activated protein kinase), JUN kinase and p38 signalling pathways implicated in control of cell proliferation and death⁴. Somatic mutations in *MAP3K1* were observed in 6% of breast cancers, predominantly in ER+ cases. Most were protein truncating. *MAP3K1* phosphorylates and activates the protein encoded by *MAP2K4*, a known recessive cancer gene with inactivating mutations in breast and other cancers⁵. In turn, *MAP2K4* phosphorylates and activates the JUN kinases *MAPK8* (also known as *JNK1*) and *MAPK9* (also known as *JNK2*), which phosphorylate JUN, TP53 and other transcription factors mediating cellular responses to stress⁴. Truncating mutations and other non-synonymous mutations were also found in *MAP3K13*, which encodes a kinase that phosphorylates and activates *MAP2K7*. *MAP2K7* phosphorylates and activates *MAPK8* and *MAPK9* (ref. 4). Thus, in breast cancer, inactivating mutations in *MAP3K1*, *MAP2K4* and *MAP3K13* are predicted to abrogate signalling pathways that activate JUN kinases (Fig. 1b).

In the serine/threonine kinase gene *AKT2*, we identified a single somatic missense mutation, Glu 17 Lys, that is identical to the recurrent, activating mutation in *AKT1* previously reported in breast cancer⁶. Thus, *AKT2* is also probably a cancer gene, albeit one infrequently implicated in breast cancer development. Because AKT phosphorylates and inhibits *MAP2K4* (ref. 7) and mutations in *PIK3CA* and *PTEN* can result in AKT activation⁸, about half of breast cancers may have abrogation of JUN kinase signalling (Fig. 1b). The biological consequences of the reduction in JUN kinase activity are likely to be diverse and complex, but may include destabilization and consequent inactivation of TP53 with disruption of pro-apoptotic cellular signalling in response to stress⁹.

We observed truncating mutations and homozygous deletions of *NCOR1*. In addition to mediating repression of thyroid-hormone and retinoic-acid receptors by promoting chromatin condensation and preventing access of the transcription machinery¹⁰, *NCOR1* participates in ligand-dependent transcriptional repression by oestrogen receptor alpha¹¹. We also identified inactivating mutations in *SMARCD1* and *ARID1B*, further implicating aberrant chromatin regulation. The encoded proteins of both are components of the SWI/SNF chromatin modelling complex, which incorporates the products of several established recessive cancer genes, including *PBRM1*, *ARID1A*, *SMARCB1* and *SMARCA4* (refs 3, 12-14).

We found three truncating mutations and a missense mutation in *CDKN1B*. Two truncating mutations in *CDKN1B* in cancer have previously been reported^{15,16}, and collectively the results confirm that *CDKN1B* is a cancer gene. *CDKN1B* (also known as p27 or KIP1) normally inhibits activation of cyclin E/CDK2 and cyclin D/CDK4 complexes, thus preventing cell cycle progression at phase G1¹⁷.

Three truncating mutations were observed in *CASP8*. *CASP8* is a member of the cysteine/aspartic acid protease family that forms a complex with the FAS cell surface receptor to promote programmed cell death. Inactivation of *CASP8* in these cancers is therefore predicted to abrogate apoptosis in response to a variety of signals.

Six tumours had mutations in *TBX3*, which encodes a T-box transcription factor that regulates stem cell pluripotency-associated and reprogramming factors and is involved in normal breast development^{18,19}. Constitutional inactivating mutations in *TBX3* cause ulnar-mammary syndrome, in which there is failure of breast and apocrine development coupled with abnormalities of limb morphogenesis²⁰. Three breast cancers had in-frame deletions, one of Thr 210 and the other two of Asn 212, a residue through which the T-box domain binds to DNA. Despite the presence of truncating mutations in three further cases, the recurrent and clustered in-frame deletions and the finding that all mutations were heterozygous suggests that they may not simply result in loss of function. Indeed, recent reports suggest that increased activity of *TBX3* is likely to contribute to oncogenesis. The proportion of stem-like cells in breast cancers is increased by oestrogen-dependent activation of the *TBX3* pathway²¹. Moreover, *TBX3* overexpression increases the efficiency of the derivation of induced pluripotent stem cells¹⁸ and the ability of cancer cells to form tumours²¹.

Further supporting their role in oncogenesis, three of the nine newly identified somatically mutated cancer genes, *MAP3K1*, *CASP8* and *TBX3*, carry inherited common variants, identified by genome-wide association studies, that confer small increased risks of breast cancer^{22,23}. Several additional genes showed truncating mutations and are biologically plausible candidate cancer genes contributing infrequently to breast cancer development. Some, including *ASXL2*, *ARID5B*, *KDM3A*, *SETD1A*, *CHD1*, *NCOR2*, *HDAC9* and *CTCF*, encode proteins that regulate chromatin structure, whereas others, including *FANCA* and *ATR*, are involved in DNA repair.

Cancers arise through successive waves of clonal expansion dependent on the sequential acquisition of driver mutations. A central parameter of cancer development is therefore the number of driver mutations required for conversion of a normal cell into a symptomatic cancer. Estimates based on cancer age-incidence curves have indicated that approximately five rate-limiting steps underlie the development of common adult solid tumours²⁴. Experimental studies have similarly indicated that a limited number of key genetic changes are required for neoplastic transformation of human cells²⁵. Our systematic genome analysis now provides a direct survey of the landscape of driver mutations in breast cancer.

Somatic driver point mutations and/or copy number changes in at least 40 cancer genes were implicated in the development of the 100 breast cancers (Fig. 2, Supplementary Tables 3 and 4, and Supplementary Methods). The maximum number of mutated cancer genes in an individual cancer was 6, but 28 cases only showed a single driver. Thus, there seems to be substantial variation in the number of drivers. In some cases, the presence of multiple drivers was associated with subclonal evolution of the cancer (Supplementary Statistical Analyses). However, in others multiple drivers were in the root cancer clone. Seven of the 40 cancer genes (*TP53*, *PIK3CA*, *ERBB2*, *MYC*, *FGFR1/ZNF703*, *GATA3* and *CCND1*) were mutated in more than 10% of cases. Collectively these contributed 58% of driver mutations (144 of 250). Therefore, 33 mutated cancer genes, each contributing relatively infrequently, were responsible for the remaining 42% of driving genetic events. We observed 73 different combinations of mutated cancer genes. Thus, most breast cancers differed from all others (Fig. 2 and Supplementary Fig. 2). This assessment of the genetic diversity of breast cancer is probably conservative because, for several reasons, it underestimates the number of mutated cancer genes in each case.

At present, we know little about the mutational processes responsible for the generation of somatic mutations in breast and other cancers. In the 100 breast cancers analysed here, there was substantial variation in the total numbers of base substitutions and indels between individual cases (Fig. 3a). There was also considerable diversity of mutational pattern, ranging from cases in which C•G → T•A transitions predominated to cases in which all transitions and transversions made equal contributions (Fig. 3b and Supplementary Fig. 3). Taken together, the results suggest that multiple distinct mutational processes are operative. For most of these processes, the underlying mechanism is unknown.

To illustrate one mutational signature in detail, we selected the ER+ breast cancer with the largest number of base substitutions in the series, PD4120 (Fig. 3a, asterisk; Fig. 4). The mutation spectrum of this case was distinctive, featuring C•G → T•A, C•G → G•C and C•G → A•T mutations and very few mutations at A•T base pairs (Fig. 4a). To characterize this process further, we examined the sequence context in which the mutations occurred (in the following discussion, mutations at C•G base pairs are represented as the change at the C base) and found pronounced overrepresentation of thymine immediately 5' to the mutated cytosines. Thus, in PD4120 the large majority of mutations were of cytosine at TpC dinucleotides (Fig. 4b).

To obtain further insight into the underlying mechanism in this case, we looked for differences in mutation prevalence between the transcribed and untranscribed strands of the 21,416 genes analysed ('strand bias') and found a higher prevalence of C→T, C→G and C→A mutations on transcribed strands ($P = 0.02$) (Fig. 4c and Supplementary Table 7). This strand bias raises the possibility that transcription-coupled nucleotide excision repair (NER) has been operative. NER removes bulky DNA adducts that distort the DNA double helix, notably pyrimidine dimers due to ultraviolet light exposure or adducts due to mutagens in tobacco smoke²⁶. There is a form of NER, recruited by RNA polymerase II, that is operative only on the transcribed strand of each gene and thus introduces a strand bias for mutations²⁷. Therefore, one hypothesis to account for the strand bias in PD4120 is past involvement of NER, in turn implicating exposure to a bulky DNA-damaging agent, either of endogenous or exogenous origin. However, we cannot exclude the possibility that other DNA damage or repair processes generate a strand bias. At least eight additional cancers in this series had a very similar mutational spectrum, sequence context and strand bias (Supplementary Fig. 4 and Supplementary Statistical Analysis). None had been treated before excision of the cancer.

The somatic mutations in a cancer genome accumulate over a patient's lifetime, during the lineage of mitotic divisions from the fertilized egg to the cancer cell. Some are acquired while cells in the lineage are biologically normal, whereas others are acquired after acquisition of the neoplastic phenotype. However, the relative proportions accumulated in these two phases are unknown. To explore this question, we examined the relationship between the total numbers of somatic base substitutions and the age at diagnosis in the 100 tumours (Fig. 5). In both ER+ and ER- cancers, no correlation was observed ($P = 0.33$ and 0.14 respectively). If most somatic mutations in a cancer genome are acquired in normal tissues before neoplastic transformation, the later the onset of the cancer the longer this part of the lineage is likely to have been and, consequently, the higher the number of mutations. The absence of a correlation there fore suggests that most mutations in breast cancer genomes occur after the initiating driver event.

We then considered separately the subset of somatic mutations constituted by C•G \rightarrow T•A substitutions at CpG dinucleotides, because this mutational pattern is observed in non-diseased tissues, manifesting prominently in normal germline variation. This subset showed a strong positive correlation with the age at cancer diagnosis in ER- cancers ($P = 1.2 \times 10^{-7}$), supporting the proposition that it is enriched in mutations occurring in normal tissues and that, overall, other mutation classes occur later. By contrast, ER+ cancers showed no correlation between C•G \rightarrow T•A substitutions at CpG dinucleotides and age at diagnosis ($P = 0.27$). The basis for this pronounced difference is unclear, but potentially highlights a profound divergence in the dynamics of mutation acquisition between these two major subclasses of breast cancer.

In clinical practice, breast cancers are graded microscopically on the basis of mitotic counts, pleomorphism of cancer cell nuclei and extent of tubule formation, which are then collected into an overall grade score. High scores indicate large numbers of mitoses, substantial tumour cell pleomorphism and little tubule formation, and are generally associated with more rapid progression. Significant correlations were not observed between numbers of driver mutations and grade scores (Supplementary Statistical Analysis). However, there were strong positive correlations between the total number of substitutions (that is, drivers and passengers) and mitosis and tubule scores ($P = 0.0002$ and 0.002 respectively), which remained significant after multiple testing corrections. The causal relationships between these features are unclear. However, because most substitutions are likely to be biologically inert passengers, it is possible that the biological state of high-grade breast cancers may be responsible for generating increased numbers of mutations, rather than the converse.

The panorama of mutated cancer genes and mutational processes in breast cancer is becoming clearer, and a sobering perspective on the complexity and diversity of the disease is emerging. Driver mutations are operative in many cancer genes. A few are commonly mutated, but many infrequently mutated genes collectively make a substantial contribution in myriad different combinations. Multiple somatic mutational processes have been operative. Ultimately, characterization of the genomes of breast cancer, and others, will provide a robust and biologically meaningful classification generating insights into the clinical heterogeneity of the disease and influencing strategies to find new modes of prevention and treatment.

METHODS

Patient samples

Informed consent was obtained from all subjects and ethical approval obtained from Cambridgeshire 3 Research Ethics Committee (ref 09/H0306/36). Collection and use of

patient samples were approved by the appropriate IRB of each Institution. In addition, this study and usage of its collective materials had specific IRB approval.

Exome enrichment and sequencing

Genomic libraries were prepared using the Illumina Paired End Sample Prep Kit following the manufacturer's instructions. Enrichment was performed as described previously³¹, using the Agilent SureSelect Human All Exon 50Mb kit following the manufacturer's recommended protocol but excluding pre-enrichment PCR amplification. Each exome was sequenced using the 75 or 76-bp paired-end protocol, on an Illumina GAI or HiSeq DNA Analyser, to produce approximately 10 Gb of sequence per exome. Sequencing reads were aligned to the human genome (NCBI build 37) using the BWA algorithm on default settings³². Reads which were unmapped, PCR-derived duplicates or outside the targeted region of the genome were excluded from the analysis. The remaining uniquely mapping reads (~60%) provided 60–80% coverage over the targeted exons at a minimum depth of $\times 30$.

Sequencing of pooled PCR amplicons

Selected genes were targeted for followup investigations in 250 additional breast cancers by sequencing of pooled PCR products. An 8-bp index was introduced during amplification to enable sequence data from individual tumours to be identified in downstream analyses.

For each amplicon, a primary PCR was performed using gene-specific primers modified with the inclusion of a common upstream adaptor sequence. A secondary PCR was performed using primers complementary to the common adaptor sequences. The reverse secondary primer contained the internal index, and 96 different indexed primers were used to enable 96 different DNAs to be pooled before sequencing. The primary and secondary PCR amplifications were performed as a simultaneous multiplex reaction. Primer sequences are available on request.

For each amplicon, PCR was performed in batches of 96 DNA samples. Following amplification, the 96 PCR products were pooled, purified using a QiaQuick column (Qiagen) and quantified on a Bioanalyser (Agilent). Pooled reactions from different amplicons (up to 50) were normalized for concentration and subsequently also pooled to produce the final template used for sequencing on a single lane of an Illumina GAI DNA Analyser (~5,000 amplicons per lane). Amplicons which failed PCR were excluded from the pooling experiments. The subsequent sequence reads were aligned with BWA and resulted in coverage typically exceeding $\times 500$ per individual sample amplicon.

Variant detection

The CaVEMan (cancer variants through expectation maximization) algorithm was used to call single nucleotide substitutions³¹. This uses a naive Bayesian classifier to estimate the posterior probability of each possible genotype (wild type, germline, somatic mutation) at each base. We applied several post-processing filters to the set of initial CaVEMan mutation calls to remove variants reported in poor-quality sequence and increase the specificity of the output.

To call insertions and deletions, we used split-read mapping implemented as a modification of the Pindel algorithm³³. This algorithm searches for reads where one end is anchored on the genome and the other end can be mapped with high confidence in two (split) portions, spanning a putative indel. Post-processing filters were applied to the output to improve specificity.

Mutations were annotated to Ensembl version 58.

Variant validation

Validation of all 7,241 putative somatic variants in the primary screen of 100 tumours and all variants found in the follow-up of 250 cases was attempted by either capillary resequencing or 454 pyrosequencing of PCR products spanning the mutation in the tumour and the normal pair. Where independent validation failed (approximately 20%) variants were reported to be somatic if manual inspection of the aligned sequence reads provided strong evidence to support their validity.

Identification of likely driver base substitutions and indels

A subset of the 7,241 substitution and indel somatic mutations identified in the exome screen were classified as 'likely driver mutations' using conservative criteria. To do this, we identified the established cancer genes from the Cancer Gene Census (<http://www.sanger.ac.uk/genetics/CGP/Census/>) that are known to be mutated by base substitutions and indels to contribute to cancer development. We then classified as likely driver mutations those that conformed to the known patterns of cancer-causing mutation for each cancer gene. Thus, for recessive cancer genes truncating mutations, essential splice site mutations and homozygous deletions were included. Missense mutations were also included where they had been seen previously or conformed to the known pattern of missense mutation in each gene (COSMIC database; <http://www.sanger.ac.uk/genetics/CGP/cosmic/>). For established, dominantly acting cancer genes, we included mutations that had been previously registered in COSMIC. For the new cancer genes established in this study, we applied essentially the same rules. However, for the recessive cancer genes, to be conservative we did not include missense variants (other than the single variant in *MAP3K1*, which is almost certainly disruptive to the function of the protein). We included the variant in *AKT2* because it is identical in nature to the recurrent variant in *AKT1*, and we included all *TBX3* mutations. As indicated in the main text, we may have both underestimated and overcalled some somatic variants as drivers using this approach. However, the number of erroneous calls is likely to be small and overall we have probably underestimated the number of driver mutations. For the calling procedure for likely driver copy number variants, see below.

Detection of copy number variation

Single nucleotide polymorphism (SNP) array hybridization on the SNP6.0 platform was done according to Affymetrix Protocols and as described at <http://www.sanger.ac.uk/cgi-bin/genetics/CGP/cghviewer/CghHome.cgi>.

Copy number analysis was performed using ASCAT (version 2.1) taking into account non-neoplastic cell infiltration and tumour aneuploidy³⁴, and resulted in integral allele-specific copy number profiles for the tumour cells. Amplifications in the 100 samples analysed were called if copy number was ≥ 5 (for diploid tumours, with ASCAT ploidy $< 2.7n$) or ≥ 9 (for tumours with evidence of a whole-genome duplication, with ASCAT ploidy $\geq 2.7n$). Homozygous deletions were called if there were zero copies in the tumour cells.

Identification of likely driver copy number variants

To identify likely driver copy number variants, we derived a conservatively generated list of frequently amplified regions in breast cancer from a previous study³⁵. From the amplified regions in breast cancer obtained by GISTIC analysis of that study, those with a GISTIC Q -value of less than 10^{-5} were selected. Regions within 40 Mb of amplified regions with more significant Q -values were excluded, as many of these probably point to the same amplified

target gene. This process generated seven focal, highly significantly amplified regions. These regions were annotated with their putative target genes where additional biological studies have indicated that they are the likely targets (*ERBB2*, *CCND1*, *MYC*, *FGFR1/ZNF703*, *ZNF217*, *MDM2*). Only the amplified region on chromosome 15 was not annotatable. Driver amplification of these seven focal regions in the 100 samples was called using the criteria above. Driver homozygous deletions were called if part or all of a homozygous deletion overlapped with a known recessive cancer gene from the Cancer Gene Census³⁶ or a newly discovered gene from this study.

Estimation of the number of mutated copies

Allele-specific copy number estimates for point mutations and indels were obtained by integrating copy number and sequencing data. In a sample containing only tumour cells, the number of reads, r , with a mutation can be expressed as

$$r = \frac{n_{\text{mut}}R}{n_{\text{locus}}} \quad (1)$$

In equation (1), n_{locus} is the copy number of the locus, n_{mut} is the number of mutated copies and R is the total number of reads from that locus. In case of a tumour sample consisting of a fraction of tumour cells ρ , infiltrated with a fraction of normal cells $1-\rho$ (assumed to have two copies), equation (1) becomes

$$r = \frac{n_{\text{mut}}R\rho}{\rho n_{\text{locus}} + 2(1-\rho)} \quad (2)$$

Hence, allele-specific copy number estimates for point mutations and indels can be obtained as

$$n_{\text{mut}} = f_s \frac{1}{\rho} (\rho n_{\text{locus}} + 2(1-\rho)) \quad (3)$$

In equation (2), $f_s = r/R$ is the frequency of mutated reads observed in the sequencing data, and ρ and n_{locus} can be obtained from the ASCAT copy number analysis.

These copy number estimates of mutations were used to determine which mutations are likely subclonal: if $n_{\text{mut}} \geq 0.8$, the mutation is called likely clonal and if $n_{\text{mut}} < 0.8$, the mutation is called likely subclonal.

In the case of indels, reads with an insertion or deletion may not map as well as reads without insertions and deletions. Therefore, a procedure was followed to estimate f_s for indels that was independent of ease of mapping. Reads were obtained by matching flanking sequence (10 bp on each side) around the indel, further filtered to exclude spurious matches. The mutated read frequency was subsequently calculated, accounting for the difference in sequence lengths with and without the indel:

$$f_s = \frac{r_{\text{indel}} / (l_s - l_{\text{indel}} + 1)}{r_{\text{indel}} / (l_s - l_{\text{indel}} + 1) + r_{\text{normal}} / (l_s - l_{\text{normal}} + 1)} \quad (4)$$

In equation (3), r_{indel} and r_{normal} are the respective numbers of reads with and without the indel, l_s is the read length (76 bp), and l_{indel} and l_{normal} are the respective lengths of the matching fragment in sequences with and without the indel.

Detection of selection and oncogenicity in protein-coding genes

The overall significance of an excess of non-silent mutations was determined using the methods previously described³⁷. The ranking of gene significances was determined using the following model. We let s_{kg}^i denote the number of silent mutations, where k indexes mutation type ($C\cdot G \rightarrow A\cdot T$, $C\cdot G \rightarrow T\cdot A$, $C\cdot G \rightarrow G\cdot C$, $T\cdot A \rightarrow A\cdot T$, $T\cdot A \rightarrow C\cdot G$ or $T\cdot A \rightarrow G\cdot C$) in gene g , where $i = 1$ for the primary screen and $i = 2$ for the follow-up screen. We also have counts m_{kg}^i and n_{kg}^i of missense and nonsense mutations, respectively. Finally we have counts l_{kg}^i of indels. The numbers of screened bases, S_{kg}^i , M_{kg}^i and N_{kg}^i , in each gene for each mutation type were also calculated. The total number of screened bases was L_g^i . We let ρ_k represent the per-base passenger mutation prevalence and use γ to denote the per-base passenger rate of indels.

Next we assume that genes can be neutral to cancer, oncogenically triggered by missense mutations or inactivated by truncating mutations. Genes are not precluded from belonging to both of the last two categories. We assume that proportions α and β of genes belong to the missense group and truncating group, respectively. Genes that belong to these groups have mutation rates that increase by factors λ and μ , respectively. These terms quantify the selection pressure for missense and truncating variants, respectively. This results in a mixture model with the following likelihood:

$$\begin{aligned} L(\rho_k, \gamma, \alpha, \beta, \lambda, \mu | s_{kg}^i, m_{kg}^i, n_{kg}^i, l_g^i) &= \prod_{g \in G} \prod_k P_{o_{s_{kg}^1}}(S_{kg}^1 \rho_k) \left(\sum_{j=1}^2 \alpha_m \prod_k P_{o_{m_{kg}^j}}(M_{kg}^j \rho_k \lambda_m) \right) \\ &\times \left(\sum_{j=1}^2 \beta_m P_{o_{l_g^j}}(L_g^j \gamma \mu_m) \prod_k P_{o_{n_{kg}^j}}(N_{kg}^j \rho_k \mu_m) \right) \\ &\times \prod_{g \in G_F} \prod_k P_{o_{s_{kg}^2}}(S_{kg}^2 \rho_k) \left(\sum_{j=1}^2 \alpha_m \prod_k P_{o_{m_{kg}^j}}(M_{kg}^j \rho_k \lambda_m) \right) \\ &\times \left(\sum_{j=1}^2 \beta_m P_{o_{l_g^j}}(L_g^j \gamma \mu_m) \prod_k P_{o_{n_{kg}^j}}(N_{kg}^j \rho_k \mu_m) \right) \end{aligned}$$

Here $\alpha_1 = 1 - \alpha$, $\alpha_2 = \alpha$, $\beta_1 = 1 - \beta$, $\beta_2 = \beta$, $\lambda_1 = 1$, $\lambda_2 = 1$, $\mu_1 = 1$ and $\mu_2 = \mu$, and $P_{o_c}(r)$ indicates the Poisson probability of obtaining value c from a Poisson process with rate parameter r . G_F denotes the set of genes in the follow-up study. The parameters for this model were then estimated with the expectation-maximization algorithm. Confidence intervals for these parameters were obtained using parametric bootstrapping. Conditional on these parameter estimates, we can then use Bayes' law to calculate the probability that each gene belongs to the neutral, the missense or the truncating group. Specifically, if $\phi_g, \psi_g \in \{1, 2\}$ index whether the gene g does or does not belong to the missense or truncating group, respectively, we have

$$\begin{aligned} \Pr(\varphi_g=m, \psi_g=n) &\propto Po_{l_g^1}(L_g^1 \gamma \mu_n) \prod_k^K Po_{s_{kg}^1}(S_{kg}^1 \rho_k) Po_{m_{kg}^1}(M_{kg}^1 \rho_k \lambda_m) \\ &\times Po_{n_{kg}^1}(N_{kg}^1 \rho_k \mu_n) \\ &\times Po_{l_g^2}(L_g^2 \gamma \mu_n) \prod_k^K Po_{s_{kg}^2}(S_{kg}^2 \rho_k) Po_{m_{kg}^2}(M_{kg}^2 \rho_k \lambda_m) \\ &\times Po_{n_{kg}^2}(N_{kg}^2 \rho_k \mu_n) \end{aligned}$$

The probability of belonging to either the missense or the truncating group, $1 - \Pr(\phi_g = 1, \psi_g = 1)$, was then used to rank the genes.

Generalized linear models

Generalized linear models (GLMs) are extensions to ordinary linear regression that model underlying distributions using members of the exponential family³⁸. The response variable is related to the linear model by a link function using maximum-likelihood estimates of the parameters. Because they are not restricted to modelling normally distributed data, GLMs have particular utility in modelling count data such as, in this manuscript, the number of mutations.

If mutations were generated by a random process, with a constant probability of occurring at any point throughout an individual's life, we would expect the number of mutations to have a Poisson distribution, dependent only on the (unknown) rate of mutation and the age of the individual. Where goodness-of-fit tests indicated that the Poisson distribution was an appropriate model for the number of mutations, we used this distribution. However, in the models where goodness-of-fit tests indicated that mutation numbers were overdispersed, we used negative binomial distributions in place of Poisson distributions, as the negative binomial distribution incorporates an additional parameter that allows the adjustment of the variance of the distribution independently of its mean.

GLMs were implemented using the `glm` and `glm.nb` functions in R. The predictor variables were {age, tumour grade, tubule score, pleomorphism score, mitotic score, mitotic count}, each of which was used within a two-factor model, with oestrogen receptor status as the second predictor variable. The response variable was the number of mutations of a particular type, from the set {substitutions 1 indels, substitutions, indels, copy number amplifications, C → T at CpG mutations, all driver mutations}.

Evaluation of strand bias in tumours displaying the mutator phenotype

To assess whether there was a strand bias of C → X (C → T, C → G and C → A) mutations in PD4120 and the other tumours showing the mutator phenotype, we first estimated the expected ratio of cytosines found in transcribed and untranscribed strands, by random sampling of 20,000 CCDS exons from Ensembl version 61. A χ -squared test was then used to examine whether the C → X mutations observed in each sample differed significantly from this ratio. Similar tests were conducted on the combined mutations from all mutator phenotype samples and on all mutator phenotype samples except PD4120.

Acknowledgments

This work was supported by the Wellcome Trust (grant reference 077012/Z/05/Z) and Breakthrough Breast Cancer. P.J.C. is personally funded through a Wellcome Trust Senior Clinical Research Fellowship (grant reference WT088340MA). P.V.L. is a postdoctoral researcher at the Research Foundation - Flanders (FWO) and is a visiting scientist at the Wellcome Trust Sanger Institute, supported by a travel grant from the FWO. I.V. is supported by a fellowship from The International Human Frontier Science Program Organization. A.-L.B.-D. and A.L. are funded

by the Norwegian Research Council, The Norwegian Cancer Society, The Radium Hospital Foundation and Health Region SØ. A.V.S. was supported by an 'Interface INSERM' grant. J.S.R.-F. is funded in part by Breakthrough Breast Cancer and is a recipient of the 2010 CRUK Future Leaders Prize. D.E. is a Principal Research Fellow of Cancer Research UK. A.T. receives financial support from the Department of Health via the National Institute for Health Research comprehensive Biomedical Research Centre award to Guy's and St Thomas' NHS Foundation Trust in partnership with King's College London, and from King's College Hospital NHS Foundation Trust in conjunction with The Experimental Cancer Medicine Centre Initiative jointly funded by Cancer Research UK, the National Institute for Health Research, the Welsh Assembly Government, the HSC R&D Office for Northern Ireland and the Chief Scientist Office, Scotland. C.D. and C.S. received partial funding from the MEDIC foundation and the Fonds National de Recherche Scientifique. J.M. and J.F. are funded in part by a research grant from the Netherlands Genomics Initiative/Netherlands Organization for Scientific Research. The INCa-Synergie facility received support from the Institut National du Cancer, the Fondation Synergie-Lyon-Cancer, the Cancropole Lyon Auvergne Rhone Alpes and the Centre Leon Berard. A.C.V. is funded by The Ludwig Institute for Cancer Research. L.v.'t.V. and A. Broeks receive funding from the Dutch Genomics Initiative-Cancer Genomics Center. We also acknowledge support for sample collection, banking and processing from the Biological Resource Center of Institut Curie; the Breakthrough Breast Cancer Unit; P. Watson and the BCCA Tumour Tissue Repository; the Centre for Translational Genomics; A. Lane and P. T. Simpson; the Australian Biospecimens Network; the Breast Unit at Royal Brisbane and Women's Hospital; the Dana-Farber/Harvard SPOR in breast cancer (reference CA089393); A. M. Sieuwerts; and the Singhealth Tissue Repository, Singapore. We are grateful also for the support of T. B. Tean, and acknowledge the input and guidance of P. Spellman and A. Ashworth.

The Oslo Breast Cancer Consortium (OSBREAC)

Rolf Karesen^{1,2}, Ellen Schlichting¹, Bjorn Naume^{2,3}, Torill Sauer^{2,4} & Lars Ottestad³

¹Department of Breast and Endocrine Surgery, Oslo University Hospital, O424 Oslo, Norway.

²Medical Faculty, University of Oslo, O424 Oslo, Norway.

³Department of Oncology, Oslo University Hospital, O424 Oslo, Norway.

⁴Department of Pathology, Oslo University Hospital, O424 Oslo, Norway.

References

1. Stratton MR, Campbell PJ, Futreal PA. The cancer genome. *Nature*. 2009; 458:719–724. [PubMed: 19360079]
2. Greenman C, Wooster R, Futreal PA, Stratton MR, Easton DF. Statistical analysis of pathogenicity of somatic mutations in cancer. *Genetics*. 2006; 173:2187–2198. [PubMed: 16783027]
3. Varela I, et al. Exome sequencing identifies frequent mutation of the SWI/SNF complex gene PBRM1 in renal carcinoma. *Nature*. 2011; 469:539–542. [PubMed: 21248752]
4. Keshet Y, Seger R. The MAP kinase signaling cascades: a system of hundreds of components regulates a diverse array of physiological functions. *Methods Mol. Biol.* 2010; 661:3–38. [PubMed: 20811974]
5. Su GH, et al. Alterations in pancreatic, biliary, and breast carcinomas support MKK4 as a genetically targeted tumor suppressor gene. *Cancer Res.* 1998; 58:2339–2342. [PubMed: 9622070]
6. Carpten JD, et al. A transforming mutation in the pleckstrin homology domain of AKT1 in cancer. *Nature*. 2007; 448:439–444. [PubMed: 17611497]
7. Park HS, et al. Akt (protein kinase B) negatively regulates SEK1 by means of protein phosphorylation. *J. Biol. Chem.* 2002; 277:2573–2578. [PubMed: 11707464]
8. Carnero A, Blanco-Aparicio C, Renner O, Link W, Leal JF. The PTEN/PI3K/ AKT signalling pathway in cancer, therapeutic implications. *Curr. Cancer Drug Targets*. 2008; 8:187–198. [PubMed: 18473732]
9. Wu GS. The functional interactions between the MAPK and p53 signaling pathways. *Cancer Biol. Ther.* 2004; 3:146–151.
10. Horlein AJ, et al. Ligand-independent repression by the thyroid hormone receptor mediated by a nuclear receptor co-repressor. *Nature*. 1995; 377:397–404. [PubMed: 7566114]

11. Merrell KW, et al. Differential recruitment of nuclear receptor coregulators in ligand-dependent transcriptional repression by estrogen receptor- α . *Oncogene*. 2010; 30:1608–1614. [PubMed: 21102521]
12. Jones S, et al. Frequent mutations of chromatin remodeling gene ARID1A in ovarian clear cell carcinoma. *Science*. 2010; 330:228–231. [PubMed: 20826764]
13. Reisman D, Glaros S, Thompson EA. The SWI/SNF complex and cancer. *Oncogene*. 2009; 28:1653–1668. [PubMed: 19234488]
14. Wiegand KC, et al. ARID1A mutations in endometriosis-associated ovarian carcinomas. *N. Engl. J. Med*. 2010; 363:1532–1543. [PubMed: 20942669]
15. Spirin KS, et al. p27/Kip1 mutation found in breast cancer. *Cancer Res*. 1996; 56:2400–2404. [PubMed: 8625318]
16. Tigli H, Buyru N, Dalay N. Molecular analysis of the p27/kip1 gene in breast cancer. *Mol. Diagn*. 2005; 9:17–21. [PubMed: 16035731]
17. Chu IM, Hengst L, Slingerland JM. The Cdk inhibitor p27 in human cancer: prognostic potential and relevance to anticancer therapy. *Nature Rev. Cancer*. 2008; 8:253–267. [PubMed: 18354415]
18. Han J, et al. Tbx3 improves the germ-line competency of induced pluripotent stem cells. *Nature*. 2010; 463:1096–1100. [PubMed: 20139965]
19. Howard B, Ashworth A. Signalling pathways implicated in early mammary gland morphogenesis and breast cancer. *PLoS Genet*. 2006; 2:e112. [PubMed: 16933995]
20. Bamshad M, et al. Mutations in human TBX3 alter limb, apocrine and genital development in ulnar-mammary syndrome. *Nature Genet*. 1997; 16:311–315. [PubMed: 9207801]
21. Fillmore CM, et al. Estrogen expands breast cancer stem-like cells through paracrine FGF/Tbx3 signaling. *Proc. Natl Acad. Sci. USA*. 2010; 107:21737–21742. [PubMed: 21098263]
22. Ghossaini M, et al. Genome-wide association analysis identifies three new breast cancer susceptibility loci. *Nature Genet*. 2012; 44:312–318. [PubMed: 22267197]
23. Varghese JS, Easton DF. Genome-wide association studies in common cancers-what have we learnt? *Curr. Opin. Genet. Dev*. 2010; 20:201–209. [PubMed: 20418093]
24. Miller D. On the nature of susceptibility to cancer. *Cancer*. 1980; 46:1307–1318. [PubMed: 7417931]
25. Schinzel AC, Hahn WC. Oncogenic transformation and experimental models of human cancer. *Front. Biosci*. 2008; 13:71–84. [PubMed: 17981529]
26. Shuck SC, Short EA, Turchi JJ. Eukaryotic nucleotide excision repair: from understanding mechanisms to influencing biology. *Cell Res*. 2008; 18:64–72. [PubMed: 18166981]
27. Fouteri M, Mullenders LH. Transcription-coupled nucleotide excision repair in mammalian cells: molecular mechanisms and biological effects. *Cell Res*. 2008; 18:73–84. [PubMed: 18166977]
28. Li H, Durbin R. Fast and accurate long-read alignment with Burrows-Wheeler transform. *Bioinformatics*. 2010; 26:589–595. [PubMed: 20080505]
29. Ye K, Schulz MH, Long Q, Apweiler R, Ning Z. Pindel: a pattern growth approach to detect break points of large deletions and medium sized insertions from paired-end short reads. *Bioinformatics*. 2009; 25:2865–2871. [PubMed: 19561018]
30. Van Loo P, et al. Allele-specific copy number analysis of tumors. *Proc. Natl Acad. Sci. USA*. 2010; 107:16910–16915. [PubMed: 20837533]
31. Varela I, et al. Exome sequencing identifies frequent mutation of the SWI/SNF complex gene PBRM1 in renal carcinoma. *Nature*. 2011; 469:539–542. [PubMed: 21248752]
32. Li H, Durbin R. Fast and accurate long-read alignment with Burrows-Wheeler transform. *Bioinformatics*. 2010; 26:589–595. [PubMed: 20080505]
33. Ye K, Schulz MH, Long Q, Apweiler R, Ning Z. Pindel: a pattern growth approach to detect break points of large deletions and medium sized insertions from paired-end short reads. *Bioinformatics*. 2009; 25:2865–2871. [PubMed: 19561018]
34. Van Loo P, et al. Allele-specific copy number analysis of tumors. *Proc. Natl Acad. Sci. USA*. 2010; 107:16910–16915. [PubMed: 20837533]
35. Beroukhi R, et al. The landscape of somatic copy-number alteration across human cancers. *Nature*. 2010; 463:899–905. [PubMed: 20164920]

36. Futreal PA, et al. A census of human cancer genes. *Nature Rev. Cancer*. 2004; 4:177–183. [PubMed: 14993899]
37. Greenman C, et al. Patterns of somatic mutation in human cancer genomes. *Nature*. 2007; 446:153–158. [PubMed: 17344846]
38. Nelder JA, Wedderburn R. Generalized linear models. *J. R. Stat. Soc. A*. 1972; 135:370–384.

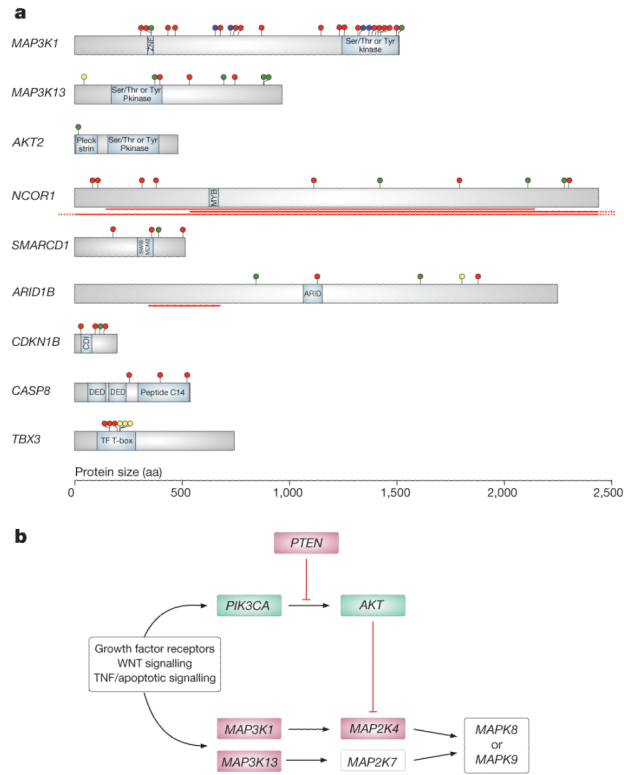


Figure 1. New cancer genes established in this study and involvement of the JUN kinase signalling pathway

a. Representations of the protein-coding sequences and major domains in cancer genes established in this study. Somatic mutations are shown as circles: truncating (red), essential splice site (blue), missense (green) and in-frame indel (yellow). The red lines indicate the positions of large homozygous deletions. aa, amino acids. **b.** Pathways regulating the JUN kinases MAP2K7 and MAP2K8, indicating genes with mutations in this series. Genes in green are activated by mutations, whereas genes in red are inactivated.

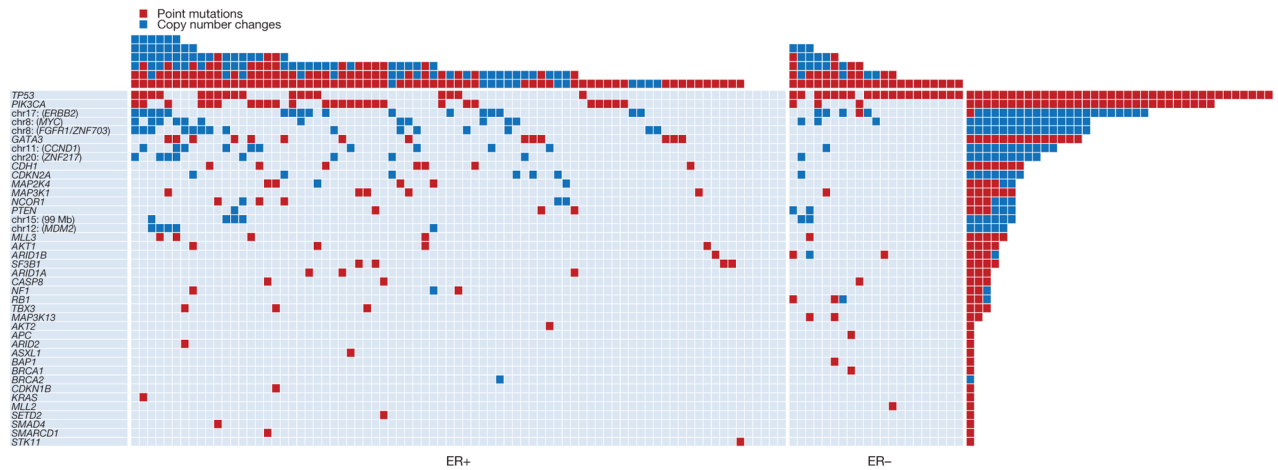


Figure 2. The landscape of driver mutations in breast cancer

Each of the 40 cancer genes in which a driver mutation or copy number change has been identified is listed down the left-hand side. The number of mutations in each gene in the 100 tumours is shown (rows), as is the number of driver mutations in each breast cancer (columns). Point mutations and copy number changes are coloured red and blue, respectively.

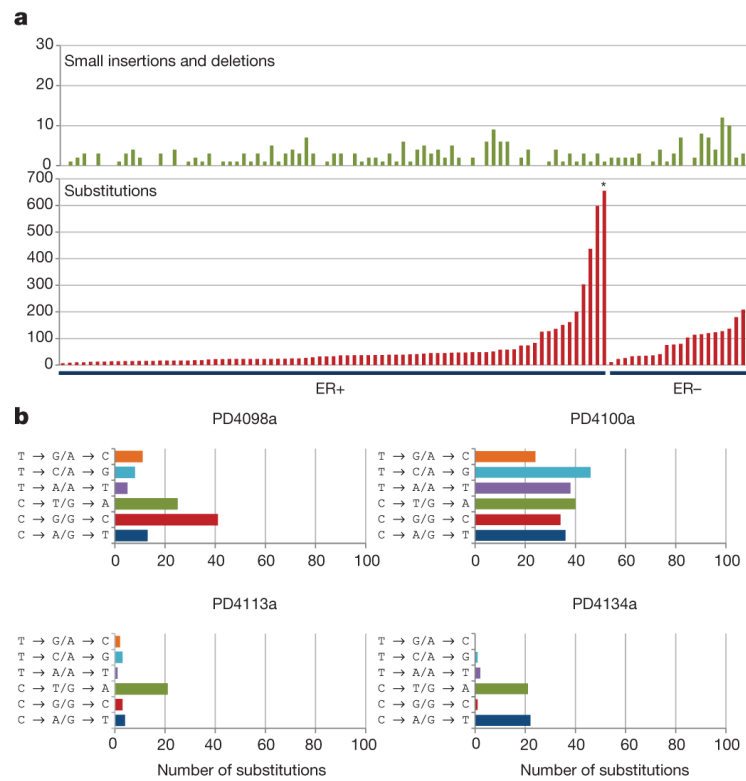


Figure 3. The variation in numbers and types of mutation between individual breast cancers
a, Numbers of small indels and base substitutions in the protein-coding exons of each of the 100 breast cancers studied. The cases are ranked according to the number of base substitutions. *Breast cancer PD4120 (see main text). **b**, Mutation spectrum of four primary tumours with diverse mutational patterns.

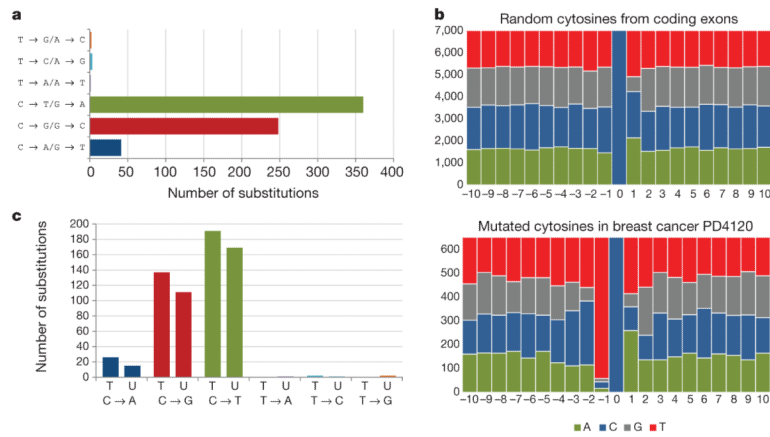


Figure 4. The mutational signature of ER1 breast cancer PD4120

a, The mutational spectrum. **b**, The sequence context of C → T, C → G and C → A mutations. The central blue bar indicates the position of the mutated cytosine and the bases 5' and 3' are numbered on the horizontal axis. **c**, Strand bias of mutations showing substitutions at C bases and at T bases according to whether they are on the transcribed (T) or untranscribed (U) strands of the genes screened.

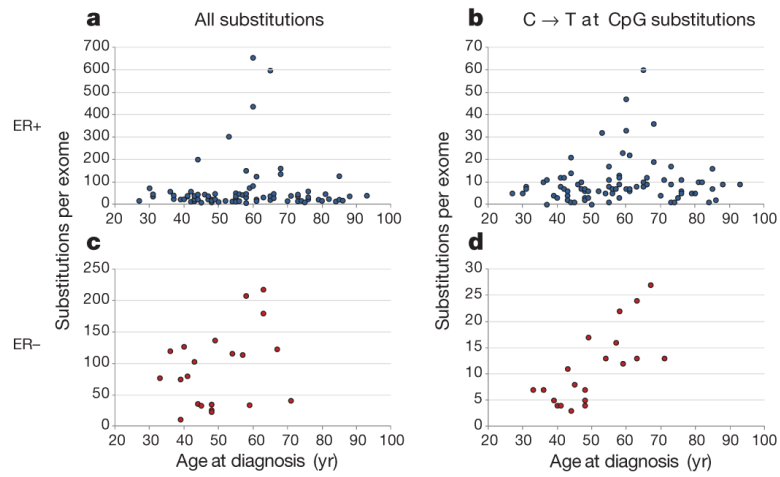


Figure 5. The relationship between age at breast cancer diagnosis and all substitutions, and for C → T substitutions at CpG sites
a, b, Data from the 79 ER+ breast cancers. **c, d,** Data from the 21 ER- breast cancers.